

Effective Knudsen Diffusivity through a Porous Solid

By Yoichi Maru* and Yoshio Kondo*

In order to measure the effective diffusivity of gas in a porous solid, the permeability was measured by using the pressure gradient technique in the pressure range between 10^{-3} mmHg and atmospheric pressure. The specimen employed was a disc-shaped porous metallic molybdenum pellet prepared by the thermal decomposition of molybdenite pellet at 1290°C in vacuum.

Below the pressure of 1 mmHg, the measured permeability converges into constant values which are 1.98, 2.40 and 6.51 cm²/sec at 15°C for Ar, N₂ and He gases, respectively. These values correspond to the effective Knudsen diffusivities of each gas and they satisfy the relationship that the effective Knudsen diffusivity is inversely proportional to the square root of molecular weight of diffusing gas. From these results, the mean pore radius is calculated at $\bar{a}=1.11 \mu$ according to the random pore model of monodisperse pore distribution.

The effective Knudsen diffusivity of diatomic sulfur gas at 1290°C in the same pellet was estimated at 3.60 cm²/sec. This value is in excellent coincidence with the estimated diffusivity of 3.52 cm²/sec which was calculated from the thermogravimetric data on the assumption that the diffusion of diatomic sulfur gas through the porous metallic molybdenum layer determines the overall rate of thermal decomposition of MoS₂ pellet.

(Received October 18, 1972)

I. Introduction

Solid-gas reactions as reduction, roasting, thermal decomposition, etc. are being employed in the process of extractive metallurgy. The porous shell of solid reaction product is formed on the surface of particles, and the rate of overall reaction is often affected by the diffusional process of gas across this porous shell^{(1)~(12)}.

Diffusion of gas through porous solid has been studied by many workers mainly in relation to the process of catalytic gas reactions, and several proposals have been made which take the pore structure into consideration^{(13)~(15)}. In the diffusional process of gas in porous solid at lower pressures or through smaller pore radii, the gas flow of the Knudsen type becomes predominant.

The present authors previously studied the rate of thermal decomposition of Mo₂S₃⁽¹¹⁾ and MoS₂⁽¹²⁾ pellets and clarified that the rate of diffusion of diatomic sulfur gas through the porous metallic molybdenum shell formed on the surface of sulfide pellet controls the overall rate of decomposition. The effective Knudsen diffusivity was also estimated from the results of thermogravimetry.

The effective Knudsen diffusivity of gas in this molybdenum shell is measured in this work by the pressure gradient technique which was proposed by Villet and Wilhelm⁽¹⁶⁾. The molybdenum pellet was prepared by the thermal decomposition of MoS₂, and the permeabilities of argon, helium and nitrogen are measured. Furthermore, the measured effective diffusivities are compared with the above-mentioned TG data.

II. Theoretical

Wakao et al.⁽¹⁴⁾ derived a rate equation for gas flow and diffusion in a capillary which is exposed in a single component gas with a pressure gradient of dP/dx . It is,

$$N = -\frac{K}{RT} \cdot \frac{dP}{dx} \quad (1)$$

where

$$K = \phi D_K + (1 - \phi) \cdot \frac{\pi}{4} D_K + (1 - \phi) \frac{a^2 P}{8\mu} \quad (2)$$

In this eq. (2), K denotes the permeability, and the right-hand side of this equation indicates the contributions of the Knudsen, slip and the Poiseuille flows to the permeability, respectively. The notation ϕ

* Department of Metallurgy, Faculty of Engineering, Kyoto University, Kyoto, Japan.

- (1) R. G. Olsson and W. M. McKewan: *Trans. Met. Soc. AIME*, **236** (1966), 1518.
- (2) N. A. Warner: *Trans. Met. Soc. AIME*, **230** (1964), 163.
- (3) L. v. H. Bogdandy, H. P. Schulz, I. N. Stranski and B. Würzner: *Ber. Bunsenges.*, **67** (1963), 959.
- (4) Y. Hara, T. Aida and S. Kondo: *J. Japan Inst. Metals*, **31** (1968), 73.
- (5) T. Otake, S. Tone and S. Oda: *Kagaku Kogaku*, **31** (1967), 71.
- (6) R. G. Olsson and W. M. McKewan: *Met. Trans.*, **1** (1970), 1507.
- (7) E. T. Turkdogan, R. G. Olsson and J. V. Vinters: *Met. Trans.*, **2** (1971), 3189.
- (8) J. Szekely and J. M. Evans: *Chem. Eng. Sci.*, **26** (1971), 1901.

- (9) A. N. Gokarn and L. K. Doraiswamy: *Chem. Eng. Sci.*, **26** (1971), 1521.
- (10) K. Natesan and W. O. Philbrook: *Trans. Met. Soc. AIME*, **245** (1969), 2243.
- (11) Y. Maru, H. Yoshida and Y. Kondo: *Trans. JIM*, **10** (1969), 8.
- (12) Y. Maru, K. Ito and Y. Kondo: *Thermal Analysis*, Academic Press, Inc., New York, vol. 2, (1969), p. 1291.
- (13) A. Wheeler: *Advances in Catalysis*, Academic Press, Inc., New York, vol. 3, (1951), p. 249.
- (14) N. Wakao, S. Otani and J. M. Smith: *AIChE Journal*, **11** (1965), 435 and 439.
- (15) R. B. Evans, III, G. M. Watson and E. A. Mason: *J. Chem. Phys.*, **35** (1961), 2076; **36** (1962), 1894.
- (16) R. H. Villet and R. Wilhelm: *Ind. Eng. Chem.*, **53** (1961), 837.

is the probability of collision of gas molecules with the capillary wall and can be expressed by

$$\phi = 1/(1 + D_K/D_{AA}). \quad (3)$$

Here the Knudsen diffusivity D_K is a function of the capillary radius, a , and the mean molecular velocity, \bar{v} , as

$$D_K = \frac{2}{3} a \bar{v} \quad (4)$$

and

$$\bar{v} = \sqrt{\frac{8RT}{\pi M}}. \quad (5)$$

The self-diffusion coefficient D_{AA} is represented by

$$D_{AA} = \frac{1}{3} \lambda \bar{v} \quad (6)$$

where λ is the mean free path of the gas molecules and it is inversely proportional to the pressure.

Furthermore, this equation for a single capillary can be extended to the gas flow in porous solid. Integrated form of eq. (1) can be rewritten as the following eq. (7) in which the permeability, K , is replaced with the effective permeability, K_e :

$$N = \frac{K_e}{RT} \cdot \frac{\Delta P}{L}. \quad (7)$$

From the random pore model in a bidisperse pore system⁽¹⁷⁾, K_e is expressed as

$$K_e = \varepsilon_a^2 \bar{K}_a + \frac{\varepsilon_i^2 (1 + 3\varepsilon_a) \bar{K}_i}{1 - \varepsilon_a}, \quad (8)$$

where the notations ε_a and ε_i are the void fractions of macro- and micropores, respectively. The permeability for macropores, \bar{K}_a , is given by a modified form of eq. (2) in which the radius, a , is replaced by the mean macropore radius, \bar{a}_a . The Knudsen diffusivity, $D_{K,a}$, can be calculated by eq. (4) where \bar{a}_a is used instead of a . It is

$$D_{K,a} = \frac{2}{3} \bar{a}_a \bar{v}. \quad (9)$$

With regard to the self-diffusion coefficient, D_{AA} , the above-mentioned effect of pressure should be taken into consideration. Similarly, the permeability for micropore, \bar{K}_i , is obtained by using the mean micropore radius, \bar{a}_i , the Knudsen diffusivity, $D_{K,i}$, and the self-diffusion coefficient, D_{AA} , respectively.

It is seen from eqs. (3) to (6) that the lowering of pressure and the decrease of pore radius yield the limiting value of collision probability of gas molecules which is equal to unity. This results in a permeability which is consistent with the effective Knudsen diffusivity, D_e . Based upon the above-mentioned considerations, it is intended in this work to obtain the effective Knudsen diffusivity of gas from the permeability measurement on a porous solid.

In the schematic illustration of Fig. 1, the porous solid pellet is placed between the two gas containers 1 and 2 whose volumes are V_1 and V_2 , respectively.

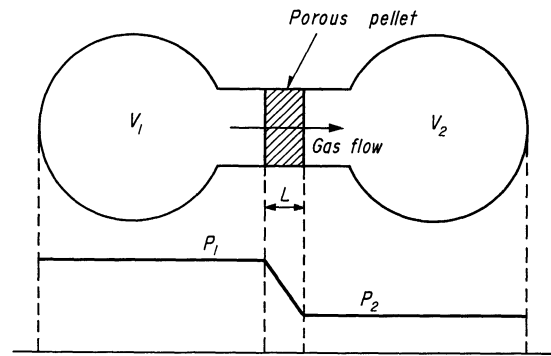


Fig. 1 Schematic illustration of permeability measurement.

The whole apparatus composes a closed system. From the mass balance equation of gas concerning both containers and the mass transfer eq. (7), we have

$$-\frac{V_1}{RT} \cdot \frac{dP_1}{dt} = \frac{V_2}{RT} \cdot \frac{dP_2}{dt} = \frac{AK_e}{RT} \left(\frac{P_1 - P_2}{L} \right), \quad (P_1 > P_2) \quad (10)$$

where A and L are the cross-sectional area and the thickness of pellet, respectively. The accumulation of diffusing gas in the pore volume of the pellet is minor in comparison with the volume of containers, and it is omitted in eq. (10). From the continuity equation in a closed system, we have

$$n_t = \frac{P_1 V_1 + P_2 V_2}{RT} = \frac{P_{10} V_1 + P_{20} V_2}{RT}. \quad (11)$$

Combination of eqs. (10) and (11) yields the following differential equation:

$$\frac{dP_2}{dt} = (G - R_v \cdot P_2) \frac{AK_e}{V_2 L}. \quad (12)$$

Integration of this equation under the assumption that K_e is constant yields

$$\log(G - R_v \cdot P_2) = -St + \log(P_{10} - P_{20}) \quad (13)$$

where

$$G = P_{10} + \frac{V_2}{V_1} P_{20}, \quad R_v = 1 + \frac{V_2}{V_1} \quad \text{and} \quad S = \frac{AK_e R_v}{2.303 V_2 L}. \quad (14)$$

Similarly, with regard to the pressure in the gas container 1, P_1 , we have

$$\log(R_v \cdot P_1 - G) = -St + \log \frac{V_2}{V_1} (P_{10} - P_{20}). \quad (15)$$

It is seen from eq. (13) that a plot of $\log(G - R_v P_2)$ against the diffusion time t yields a linear relationship whose slope is equal to $-S$. From this slope, the permeability K_e is calculated by the following equation:

$$K_e = \frac{2.303 L V_2}{A R_v} \cdot S_{\text{obs.}} \quad (16)$$

III. Experimental

1. Experimental apparatus and the procedure

The experimental apparatus was designed to measure the permeability in the pressure range be-

(17) N. Wakao and J. M. Smith: Chem. Eng. Sci., 17 (1962), 825.

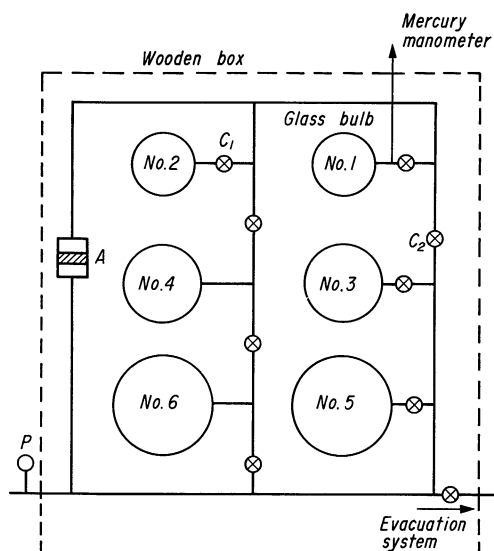


Fig. 2 The schematic allocation of experimental apparatus.

tween one atmosphere and about 10^{-3} mmHg. It is schematically illustrated in Fig. 2. As seen in the figure, it is composed of six glass bulbs of Nos. 1 to 6, a diffusion cell A, a Pirani gauge P which is connected to the downstream of the diffusion cell, and an evacuation system S. The whole apparatus except the Pirani gauge and the evacuation system is enclosed within a wooden box which is lined with the styrofoam plate of 2 cm thickness in order to avoid the temperature variation during the measurement. And the temperature can be maintained within $\pm 0.5^\circ\text{C}$ during each experimental run.

Table 1 Volumes of glass bulbs.

No.	1	2	3	4	5	6
Volume (cm ³)	1375	1228	2484	2589	4204	4182

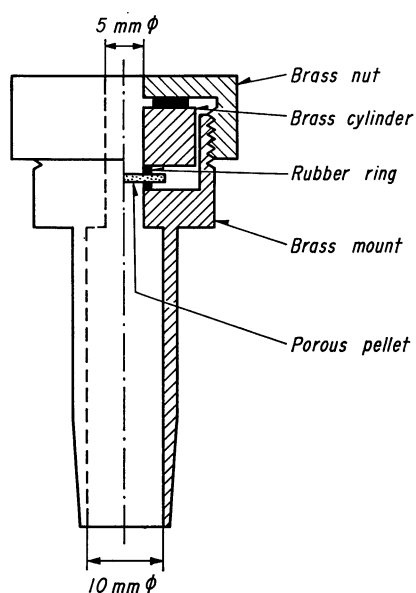


Fig. 3 Diffusion cell.

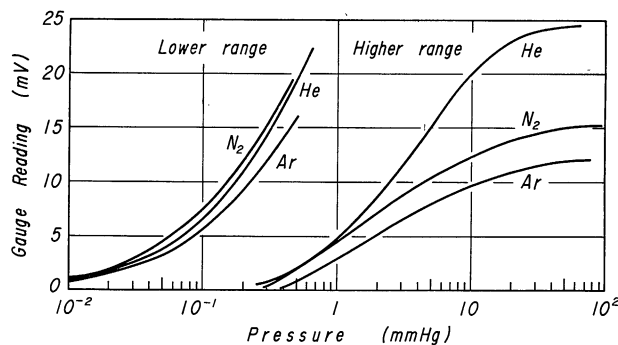


Fig. 4 Calibration curve of Pirani gauge for Ar, N₂ and He gases.

The volume of glass bulbs Nos. 2 to 6 was measured by using a mercury manometer. The glass bulb No. 1 was taken as the reference whose volume was exactly measured beforehand. It is 1375 cm³ at 15°C. And the volume of other glass bulbs are summarized in Table 1.

Details of the diffusion cell are shown in Fig. 3. A porous pellet is held between two rubber rings which are tightened with the screw of the brass mount. The inner diameter of the rubber rings was adjusted to be the same as the opening of the mount.

The measurement of pressure is conducted by means of the Pirani gauge. Before the measurement of permeability, the sensitivity of this gauge was tested with argon, helium and nitrogen gas. The result is shown in Fig. 4.

The measurement of pressure changes caused by the diffusion through porous pellet was conducted as follows: gas is introduced into the glass bulb of upper stream and the pressure is adjusted to a fixed value of P_{10} . The downstream glass bulb is evacuated to the pressure of P_{20} . The upper stream and downstream are separated by closing the valve C_2 . The whole space of the apparatus is then isolated from the evacuation system. The measurement of pressure change is started by opening the valve C_1 , and the increase of the downstream pressure is recorded.

2. Material

The sample pellet employed in this work is a disc-shaped porous metallic molybdenum which was prepared by the thermal decomposition of a MoS₂ pellet: MoS₂ powder of -300 mesh size was pressed into a disc-shaped pellet at a pressure of 94 kg/cm² and then decomposed into metallic molybdenum in vacuum at 1290°C. The porous metallic molybdenum pellet thus prepared is 0.176 cm high and 1.14 cm in diameter. The porosity is estimated at 0.83. Furthermore, the effective Knudsen diffusivity of S₂ gas through this pellet at 1290°C was estimated in the previous paper⁽¹²⁾ at 3.52 cm²/sec.

3. Experimental results

First, the possible transport resistance along the glass tubing between glass bulbs in the measuring apparatus was examined. Before the permeability measurement of the pellet, the conductances of the

Table 2 Permeability obtained from various combinations of glass bulbs.

Bulb number (higher pressure side)	Bulb number (lower pressure side)	Permeability (cm ² /sec)	
		N ₂	Ar
No. 2	No. 5	2.40	1.96
	No. 6	2.42	1.98
	No. 5+6	2.33	2.05
	No. 3	2.51	—
No. 4	No. 5	2.40	—
	No. 6	2.43	—
	No. 5+6	2.34	—

pellet and the glass tubing installed between the glass bulbs were estimated. It was revealed from this calculation that the resistance of glass tubing is less than 5% of the pellet and the former resistance can be omitted. In order to further ascertain this calculation, the permeability measurement was carried out by employing several combinations of the glass bulbs installed at different positions.

Experimental results with nitrogen and argon are summarized in Table 2. It is supposed from the allocation of glass bulbs that the resistance is highest in the combination of bulbs Nos. 4 and 5 and it is lowest in the combination of Nos. 2 and 6. As seen in Table 2, however, the whole experimental data are consistent within an error of 5%, and it can be said that there is no significant difference by the different combination of glass bulbs. In the following measurements, therefore, a combination of glass bulbs Nos. 2 and 6 (Nos. 5 and 6 in a few runs) was employed.

Argon, helium and nitrogen gases were used as the diffusing gas in the permeability measurement. Figure 5 demonstrates, as an example, the plot of $\log(G - R_v P_2)$ against the diffusion time which is based on eq. (13). Argon was employed as the diffusing gas in this experiment. As seen in the figure, the linearity of the line was found to be excellent over the whole range of measurement. The mean pressure defined by $\bar{P} = (P_1 + P_2)/2$ is also illustrated in the same

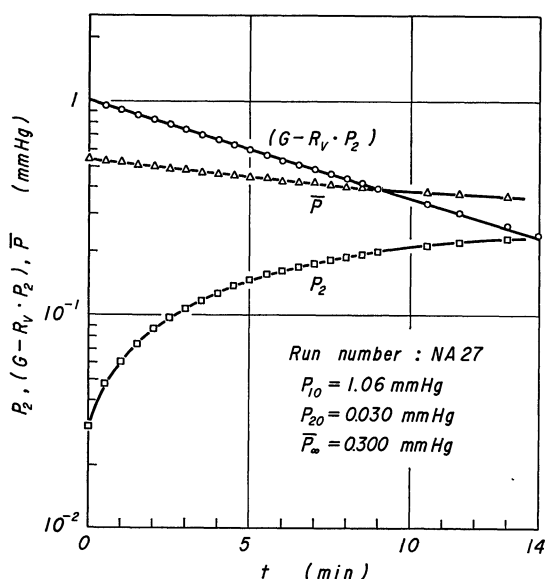


Fig. 5 An example of time-variation curves of P_2 , \bar{P} and $(G - R_v P_2)$ with argon at 15°C.

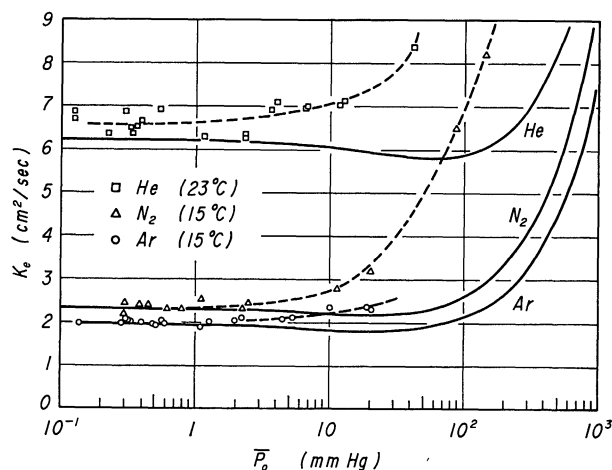


Fig. 6 Permeabilities of Ar, N₂ and He gases. (dotted line: observed values, solid line: calculated values)

figure. Because the volume ratio, V_2/V_1 , of glass bulbs employed in this measurement is not unity, \bar{P} gradually decreases along the course of diffusion.

The permeabilities were calculated from the slope of a straight line shown in Fig. 5 and are summarized in Fig. 6. As mentioned above, the mean pressure \bar{P} changes along with the diffusion time, and the permeability is plotted against the initial mean pressure \bar{P}_0 ; it is supposed that the permeability is not significantly affected at low pressures.

At lower pressures, the Knudsen flow becomes predominant over the Poiseuille flow. In the pressure region below 1 mmHg, the response of Pirani gauge is very rapid (within several seconds) even when the initial pressure difference is large. However, the response becomes slower with increasing pressure above a few mmHg. Accordingly, the permeability data in the pressure region of 1 mmHg and above shown in this figure are thought to be somewhat unreliable.

As seen in Fig. 6, the permeability of each gas remains unvaried below about 1 mmHg. This is expected from eq. (2) and these values of permeability correspond to the effective Knudsen diffusivity of each gas. Their mean values are 1.98 and 2.40 cm²/sec for argon and nitrogen at 15°C, respectively, and 6.60 cm²/sec for helium at 23°C.

IV. Discussion

The effect of the molecular weight of diffusing gas on the Knudsen diffusivity is demonstrated by eqs. (4) and (5). D_K is inversely proportional to the square root of molecular weight and is proportional to the square root of absolute temperature. These relationships are also valid for the effective Knudsen diffusivity, and the ratio of effective Knudsen diffusivities of gases A and B of different molecular weight can be expressed by the following equation:

$$\frac{D_{e,B}}{D_{e,A}} = \frac{D_{K,B}}{D_{K,A}} = \sqrt{\frac{T_B M_A}{T_A M_B}} \quad (17)$$

Table 3 Effect of molecular weight of diffusing gas on permeability.

Gas	Molecular weight	D_e (cm ² /sec)	$(D_{e,B}/D_{e,Ar})_{obs.}$	$(D_{e,B}/D_{e,Ar})_{cal.}$
Ar	40	1.98	1	1
N ₂	28	2.40	1.21	1.20
He	4	6.51	3.29	3.16

The ratio of the measured effective diffusivities is compared with the ratio calculated by this equation, as shown in Table 3. It is seen that the coincidence between the diffusivities of argon and nitrogen is excellent within the experimental error. However, in regard to helium gas, the ratio of the observed diffusivities seems to be a little higher than the calculated one. This may be due to the delay in the response of the Pirani gauge at higher flow rates of helium gas.

In order to predict the effective permeability, K_e , from eq. (8), the values of void fractions, ϵ_a and ϵ_i , and mean pore radii, \bar{a}_a and \bar{a}_i , for macro- and micropores, respectively, must be obtained, for which it is further necessary to measure the pore radius distribution within the pellet. However, since the measurement of the pore radius distribution was not conducted in this work, we tried to calculate the overall mean pore radius, \bar{a} , from the permeability data obtained. Under the assumption that the pores in the pellet is composed of monodisperse macropores only, eq. (8) is simplified to

$$K_e = \epsilon^2 \bar{K}. \quad (18)$$

This assumption is thought to be valid in this pellet because of such a fairly large void fraction as 0.83. In the Knudsen flow region, $D_K \ll D_{AA}$, or $\phi = 1$. This relationship yields very simple equations of $\bar{K} = D_K$ and $K_e = D_e$. And eq. (18) is again rewritten as

$$D_e = \frac{2}{3} \epsilon^2 \bar{a} \sqrt{\frac{8RT}{\pi M}}. \quad (19)$$

Presuming that argon is employed as the diffusing gas, the following data are substituted into eq. (19).

$$\epsilon = 0.83$$

$$T = 288^\circ \text{K}$$

$$M = 40 \text{ and}$$

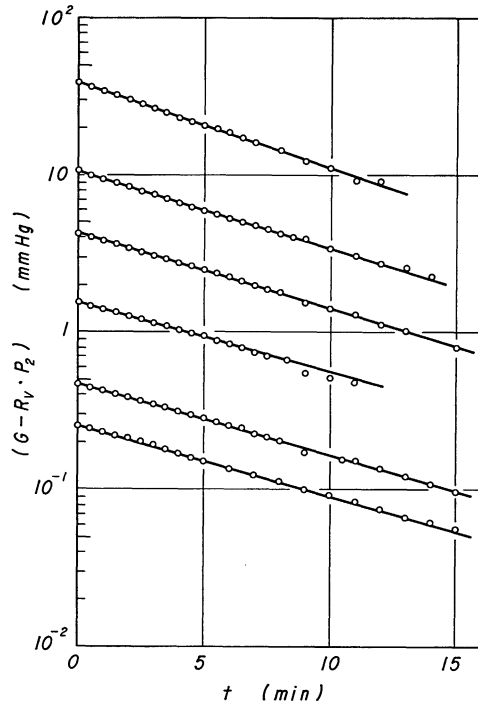
$$D_e = 1.98 \text{ cm}^2/\text{sec}.$$

And we have $\bar{a} = 1.11 \times 10^{-4}$ cm.

Based on these calculations, it also becomes possible to predict the effect of pressure on the effective diffusivity. In order to take the effect of mean pressure, \bar{P} , into consideration, eq. (2) was substituted into eq. (18) and the following equation was obtained:

$$K_e = \epsilon^2 \phi \bar{D}_K + \epsilon^2 (1 - \phi) \frac{\pi}{4} \bar{D}_K + \epsilon^2 (1 - \phi) \frac{\bar{a}^2 \bar{P}}{8\mu} \quad (20)$$

in which the mean pore radius, \bar{a} , is employed. By using this equation, the effective permeability was calculated as the function of pressure, and the results are also demonstrated with solid lines in Fig. 6. It is seen in this figure that both measured and calculated permeabilities increase at higher pressures, evidently

Fig. 7 Log $(G - R_v P_2)$ vs. t curve with argon gas (15°C).

because of the increased contribution of the Poiseuille flow, or the third term on the right-hand side or eq. (20).

However, it is seen in this figure that both diffusivities do not coincide at higher pressures with each other. It has already been mentioned that the mean pressure is not maintained constant but gradually changes during the measurement. In order to further make clear the above-mentioned disagreement, the plot of $\log(G - R_v P_2)$ vs. t with argon gas was again examined, as illustrated in Fig. 7.

Although the mean pressure is not maintained constant in this measurement, excellent linear relationships are observed in this figure even in the higher pressure region. This suggests that eq. (13) can also be applied in the higher pressure region. And it is also predicted that the disagreement between the measured and calculated permeabilities at higher pressures may be caused by the delayed response of the Pirani gauge in this pressure region.

This prediction also leads to a conclusion that only the experimental results obtained at lower pressures can be compared with the theoretical values. No further mention will be made of the results obtained at higher pressures (above about 1 mmHg).

Finally, the effective Knudsen diffusivity of diatomic sulfur gas through the porous metallic molybdenum pellet was estimated at 1290°C and compared with the estimated value from the result of thermogravimetry. The conversion of the diffusivity obtained in this work into the value under the conditions of thermal decomposition was carried out by using eq. (17). This equation can be rewritten as

$$\frac{D_{e,S_2}}{D_{e,Ar}} = \sqrt{\frac{T_1 M_{Ar}}{T_2 M_{S_2}}}. \quad (21)$$

By substituting $T_1 = 1523^\circ\text{K}$, $T_2 = 288^\circ\text{K}$, $M_{\text{S}_2} = 64$, $M_{\text{Ar}} = 40$ and $D_{e,\text{Ar}} = 1.98 \text{ cm}^2/\text{sec}$, we have $D_{e,\text{S}_2} = 3.60 \text{ cm}^2/\text{sec}$ at 1290°C which is very close to $3.52 \text{ cm}^2/\text{sec}$ obtained from the TG data. This calculation may also suggest that the rate of thermal decomposition of the molybdenite pellet at 1290°C in vacuum is controlled by the diffusional process of diatomic sulfur gas through the porous metallic molybdenum shell formed.

V. Summary

The effective diffusivity of gas through porous solid was measured by using the pressure gradient technique. The permeability was measured in the pressure range between 10^{-3} mmHg and atmospheric pressure. The specimen was a disc-shaped porous metallic molybdenum pellet which was prepared by the thermal decomposition of molybdenite pellet at 1290°C in vacuum.

At lower pressures below 1 mmHg, the precision of the permeability measurement was excellent and the dispersion of permeability data obtained was within 5%.

The effective Knudsen diffusivities of argon, nitrogen and helium gases were estimated at 1.98, 2.40 and $6.51 \text{ cm}^2/\text{sec}$ at 15°C , respectively. And the theoretical relationship of diffusivity among these gases of different molecular weight was also satisfied. From the results of permeability measurements, mean pore radius in this metallic molybdenum pellet was estimated to be $\bar{a} = 1.11 \times 10^{-4} \text{ cm}$.

Because of the pore characteristics of the pellet, the permeation of gas was fairly rapid. And the obtained permeability above about 1 mmHg was not so accurate, because of the slower response of the Pirani gauge at higher pressures.

The effective Knudsen diffusivity of diatomic sulfur gas through this pellet was estimated at $3.60 \text{ cm}^2/\text{sec}$ at 1290°C . This value is in excellent coincidence with the estimated diffusivity of $3.52 \text{ cm}^2/\text{sec}$ which was calculated from the thermal decomposition rate of the molybdenite pellet on the assumption that the diffusional process of diatomic sulfur gas through the metallic molybdenum shell controls the overall rate

of decomposition.

Acknowledgment

The authors are very grateful to Messrs. A. Tsuchida and A. Inoue for their help in the permeability measurements.

Notation

A : cross-sectional area of pellet for gas flow	[cm^2]
a : pore radius	[cm]
D_K : Knudsen diffusivity	[cm^2/sec]
D_{AA} : self-diffusion coefficient	[cm^2/sec]
G : constant	[—]
K : permeability	[cm^2/sec]
L : thickness of pellet	[cm]
M : molecular weight	[g/mol]
N : flux of gas flow	[$\text{mol}/\text{cm}^2 \cdot \text{sec}$]
n_t : total number of moles	[mol]
P : pressure	[atm]
ΔP : pressure difference	[atm]
R : gas constant ($= 1.987$)	[$\text{cal}/\text{mol} \cdot ^\circ\text{K}$]
R_v : dimensional constant ($= 1 + V_2/V_1$)	[—]
S : slope of a straight line	[—]
T : absolute temperature	[$^\circ\text{K}$]
t : diffusion time	[sec]
V : volume of glass bulb	[cm^3]
v : mean molecular velocity	[cm/sec]
x : length of diffusional path in the pellet	[cm]

Greek letters

ε : void fraction	[—]
λ : mean free path	[cm]
μ : gas viscosity	[$\text{g}/\text{cm} \cdot \text{sec}$]
ϕ : probability factor	[—]

Subscript

a, i : macro- and micropores, respectively
1, 2: higher and lower pressure sides of pellet, respectively
0: initial value
e : effective value